



Investigation of electrochemical degradation of Basic Red 13 dye in aqueous solutions based on COD removal: numerical optimization approach

D. Ozturk¹ · A. E. Yilmaz²

Received: 1 October 2019 / Revised: 15 February 2020 / Accepted: 19 February 2020 / Published online: 28 February 2020
© Islamic Azad University (IAU) 2020

Abstract

The aim of this study was to remove Basic Red 13 dye by electrochemical oxidation with Ti/Pt anodes and to numerically optimize the operating conditions such as current density (5–20 mA/cm²), flow rate (10–50 mL/min), initial pH (2–9) and supporting electrolyte concentration (10–100 mM) by using response surface methodology. Chemical oxygen demand analysis which was chosen as a response was performed according to closed reflux colorimetric method. Also, the effluent chloride levels were analyzed with the argentometric method. Momentary temperature, pH and electrical conductivity readings were taken with a multimeter. Although a number of possible system conditions were obtained with numerical optimization, the system operating conditions with the lowest energy consumption are considered to be optimal. From the quadratic model formed from central composite design in response surface methodology with numerical analysis, the optimum conditions were determined to be 4.38 for initial pH, 19.53 mA/cm² for current density, 40.78 mL/min for flow rate and 85.57 mM for supporting electrolyte concentration. At these optimum points, chemical oxygen demand removal efficiency was calculated as 99.98% and energy consumption values of the system were calculated as 7.91 kW h/m³ and 0.98 kW h/kgCOD. Under these conditions when an industrial system is operated, the chemical oxygen demand removal yield will be 99.98% and the approximate cost of the system will be \$1.25 to treat 1 ton of wastewater.

Keywords Basic Red 13 · Cationic dye · Electrochemical oxidation · Response surface methodology

Introduction

Dye stuffs are widely used in many industries, such as paint, paper, textile and leather which produce colored products. More than 10,000 commercial dyes are available, and an average of 7×10^5 tons of dye-containing wastewaters is produced annually (Qada et al. 2006; Kaykioglu and Debik

2006; Wang et al. 2008). In addition to causing esthetic pollution, they create turbidity in the aquatic environment and prevent sunlight from penetrating into the water and adversely affect the photosynthesis reactions which are important for aquatic plants (Wang et al. 2005; Qada et al. 2006).

Many alternative processes for the treatment of wastewater containing dyes have been reported in the literature such as adsorption (Ozturk et al. 2017; Ilgin and Ozay 2017), biological treatment (Sarvajith et al. 2018; Bahia et al. 2018), chemical coagulation (Tiaiba et al. 2018; Dotto et al. 2019), membrane filtration (Hassani et al. 2008; Khumalo et al. 2019), ozonation (Gharbani et al. 2008; Venkatesh and Venkatesh 2019) and electrochemical treatments (Vignesh et al. 2014; Assémian et al. 2018; Şen et al. 2018). One of the important points in wastewater treatment is that the treatment method to be applied should be a process that does not produce secondary waste. It is not considered an environmentalist approach to remove pollutants from wastewater

Editorial responsibility: M. Abbaspour.

Electronic supplementary material The online version of this article (<https://doi.org/10.1007/s13762-020-02692-2>) contains supplementary material, which is available to authorized users.

✉ D. Ozturk
dozturk@yyu.edu.tr

¹ Department of Environmental Engineering, Faculty of Engineering, Van Yuzuncu Yil University, Van, Turkey

² Department of Environmental Engineering, Faculty of Engineering, Ataturk University, Erzurum, Turkey



and move them to another environment. It is also important that the treatment method is effective and economical.

One of the treatment methods that can be applied in this respect is the electrochemical oxidation (EO) process. Compared with conventional and other advanced oxidation process (AOP) methods, the EO process involves no secondary waste generation and no variation problems for the anode (Ozturk and Yilmaz 2019). EO is an environmentally friendly technology that can fully mineralize organic materials that are not completely biodegradable (Brillas and Martínez-Huitle 2015). The reaction can be easily terminated in seconds by disconnecting electrical power and then restarted quickly. EO can be used to remove many contaminants and can process quantities from microliters to millions of liters (Anglada et al. 2009). Furthermore, EO generally has lower temperature and pressure requirements than equivalent non-electrochemical techniques, such as supercritical oxidation (Anglada et al. 2009). The main disadvantage of this process is the high operating cost due to high energy consumption. The solution is to decrease ohmic resistance to decrease cell voltage with cell design optimization (Zhu et al. 2009). Also, Takdastan et al. (2015) and Atmaca (2009) reported that distance between electrodes strongly affected the energy consumption of the system. Passivation, abrasion and polarization of the electrodes are other disadvantages. These problems can be ameliorated by developing advanced plate materials or selecting durable anodes like boron-doped diamond (BDD) electrodes, mixed metal oxide (MMO) electrodes, etc. In addition, wastewater must be electrically conductive in order to apply this technology. The EO process is advantageous for industrial wastewaters since they have good electrical conductivity.

The aim of this study is to remove Basic Red 13 (BR13) dye from aqueous solutions by EO with Ti/Pt anodes and to optimize the operating conditions (current density (CD, J), flow rate (Q), initial pH and supporting electrolyte (SE) concentration) by using response surface methodology (RSM).

Based on the author's knowledge, although several studies examined electrochemical treatments of dye-containing wastewaters, there is no study about the investigation and optimization of EO of BR13 dye wastewater with Ti/Pt anodes.

Materials and methods

Dye solution, analyses and calculations

In this study, BR13 dye was used for the preparation of aqueous solutions. General characteristics of BR13 are given in Table S1 (Online Resource 1). Dye solution concentrations were fixed at 100 mg/L for all experiments. Because of its low electrical conductivity, distilled water

was not used for solution preparation, so tap water was used for the preparation of solutions. Tap water which was used in experiments contains chlorides, nitrates, sulfates and bicarbonates with concentrations of 1.20 mg/L, 1.50 mg/L, 7.50 mg/L and 110 mg/L, respectively.

System efficiency was determined based on chemical oxygen demand (COD) removal (Eq. 1) (Ozturk and Yilmaz 2019). The COD of the solution was analyzed using a spectrophotometer (WTW Spektroflex 6100) at a wavelength of 600 nm according to the closed reflux colorimetric method (Eaton et al. 1995). Momentary temperature, pH and electrical conductivity readings were taken with a multimeter (WTW multi340i).

$$Y_o(\%) = \frac{(C_0 - C_t)}{C_0} \times 100 \quad (1)$$

C_0 and C_t represent the concentrations before oxidation ($t=0$ min) and after oxidation at time t , respectively. Y_o represents the experimentally observed removal yield of BR13 as an expression of COD. Since the chloride content in the solution was high because additional NaCl was used, the effluent chloride levels were analyzed with the argentometric method (Ademoroti 1996). To calculate the chloride concentration of effluents, Eq. 2 (Ademoroti 1996) was used:

$$(\text{Cl}^-) \left(\frac{\text{mg}}{\text{L}} \right) = \frac{(V_t - V_b) \times N_t \times 1000 \times 35.5}{V_s(\text{mL})} \quad (2)$$

V_t represents the amount of AgNO_3 consumed in the titration for the sample (mL), V_b represents the amount of AgNO_3 consumed in the titration for the blank (mL), N_t represents the normality of AgNO_3 , and V_s represents the sample volume (mL).

With the use of Eq. 3 (Rahmani et al. 2015) and Eq. 4 (Azarian et al. 2018), energy consumption (E) values were determined.

$$E \left(\frac{\text{kWh}}{\text{m}^3} \right) = \frac{V \times I \times t}{v} \quad (3)$$

Here, V (Volt) is the electric potential, v (m^3) is the volume of dye solution, I (ampere) is the electric current, and t (hour) is the reaction time. Using Eq. 4, the specific energy consumption (SEC) of the system was determined per kg of degraded COD:

$$\text{SEC} \left(\frac{\text{kWh}}{\text{kg COD}} \right) = \frac{V \times I \times t}{\Delta C \times V_R} \quad (4)$$

Here, ΔC is the difference in inlet and outlet concentration of COD (mg/L) of the sample taken at the time of reaction, and V_R is the volume of dye solution (liter).

Characteristics of the Ti/Pt anode

Ti/Pt mesh type electrodes utilized in this study were commercially obtained (Umicore). Commercially available electrodes were used in experiments without any treatment. However, to know how these electrodes are prepared and processed gives the experimenter information about the durability of the electrodes. The electrode was prepared by coating Pt on a Ti layer. The platinum coating is applied by means of high-temperature electrolysis (HTE) (Dick 1990). The platinum is deposited from a cyanide molten salt bath at temperatures of 500 to 600 °C. Mesh type pure Ti electrodes were supplied in plate form, and electrodeposition was performed in molten medium containing NaCN (48%) and KCN (50%). During the electrodeposition process, Pt (1–3%) was used in pure form and dissolved in cyanide molten medium; then, electrodeposition was performed in the cell which was closed under vacuum with argon gas. During the coating process, the temperature was gradually increased to 500–600 °C. Other operating conditions during the Pt coating process are as follows: cathodic current density 1–5 A/dm², deposition rate 10–50 μm/h, deposition voltage 1–2 V. Also, SEM, EDX and plasticity analyses of Ti/Pt anode were performed with ZEISS GeminiSEM 300 model analyzer.

Experimental setup

A glass-jacketed cylinder reactor (height 22 cm, radius 3.5 cm) was used for the circulation of cooler liquid to fix the reaction temperature at 25 °C with a liquid circulator (Labo C200-H13). Three cathodes (Ti) and three anodes (Ti/Pt) with mesh type were connected to direct current (DC) power supply (TTI/QPX1200S) with a monopolar parallel connection. The gap between the electrodes was 3 mm. Each electrode was 40 mm × 200 mm, and the total surface area of electrodes was 1056 cm². A magnetic stirrer (Daihan-Brand) was utilized to prevent precipitation of dye particles in solution. A peristaltic pump (Masterfleks R/S) was used to adjust the flow rate of solutions. For all experiments, wastewater volume was fixed at 700 mL.

Design of experiments

RSM is a unique method that includes experimental methods to examine the experimental space of process variables, while empirical modeling methods are used to determine the relationship between the response of the process and the independent variables acting on it. It is also a preferred technique for determining levels at which system variables have the desired effect on the response of the system. The four system variables, namely initial pH (A), J (B), Q (mL/min) (C) and SE concentration (mM) (D), were selected for

Table 1 Value ranges for CCD experiments

Independent parameters	Uncoded and coded values		
	−1	0	+1
Initial dye solution pH (A)	2	5.50	9
Current density (<i>J</i> , mA/cm ²) (B)	5	12.50	20
Flow rate (<i>Q</i> , mL/min) (C)	10	30	50
SE concentration (mM) (D)	10	55	100

COD removal yield (%) which is the response. CCD is a procedure that provides system optimization by explaining the relationship between dependent and independent variables and revealing to what extent the effect of the independent variables and the interaction of the factors have a significant effect on the response variable. Thirty experimental sets were proposed by CCD according to the equation $2^k + 2k + 6$ (k is 4 for this study). Six experiments were performed at the central points (0) to reveal the experimental error. Each value for the independent parameters was entered into the system as the highest (+1) and lowest (−1) points (Table 1). Apart from the independent system variables, there are also parameters that are kept constant in the system; these are: initial BR13 concentration 100 mg/L and reaction temperature 25 °C.

The quadratic function, which explains the relationship between the dependent and independent variables, is given in Eq. 5 (Öztürk and Şahan 2015; Kıvanç and Yönten 2020):

$$\hat{y}_n = \beta_0 + \sum_{i=1}^n \beta_i x_i + \sum_{i=1}^n \beta_{ii} x_i^2 + \sum_{i=1}^n \sum_{j=i+1}^n \beta_{ij} x_i x_j \quad (5)$$

where β_0 is the constant response value at the center of the design; β_i , β_{ii} and β_{ij} are linear, quadratic (quadratic) and interactive effect of regression terms, respectively; X_i is the level of the independent factor; n (4 in this study) is the number of independent factors; ε is the random error. In order to obtain the interaction between the responses and the variables, Eq. 5 was analyzed using the Design-Expert 7.0.1 program, which includes the ANOVA test, and the suitability of the model was expressed with R^2 .

Results and discussion

Structural properties of Ti/Pt anode

The Pt deposition surface consists of stacks of approximately prism-like structures with sizes ranging from nano-scales to micron size. The cross-sectional image and SEM image of the anode are shown in Fig. 1a, b, respectively. As a result of this situation, the electrode has a porous structure and so has a high surface area. The total surface area of the mesh



Fig. 1 SEM cross section, etched (a), SEM image (b) of Ti/Pt anode surface

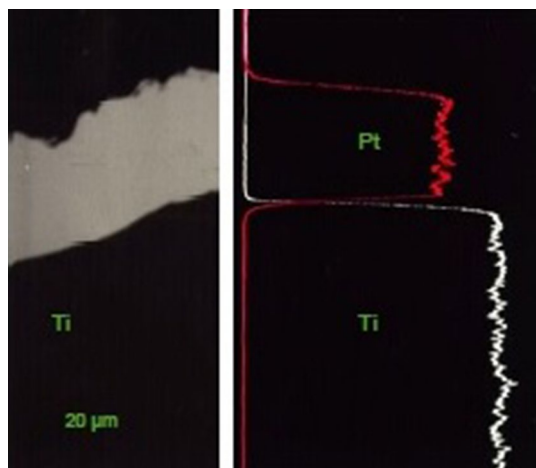
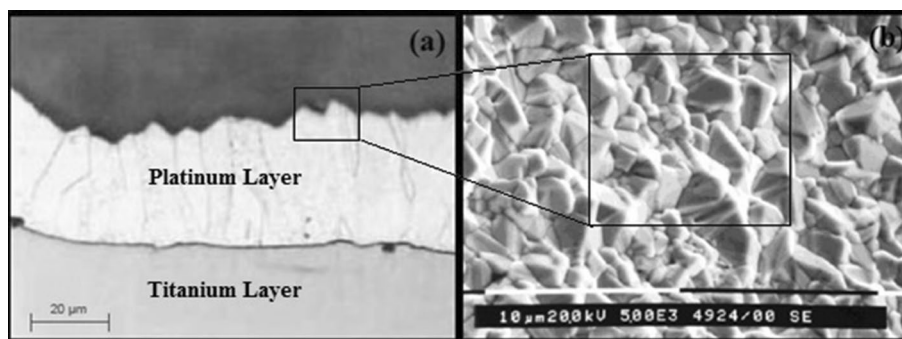


Fig. 2 Cross section and EDX X-line scan image

type electrode used was calculated as 1056 cm^2 . Mesh type electrodes are superior to plate-shaped electrodes due to increasing contact area of the solution and electrode surface. At the same time, the concentration of all oxidants, which are the main drivers of oxidation, increases with the increased surface area; on the other hand, the surface for chemisorbed oxygen which contributes less to oxidation is enhanced so mesh type electrodes have a great advantage in terms of process efficiency. Ti/Pt electrodes obtained with HTE technique are resistant to experimental conditions. Physical properties of the electrode such as ductility, hardness, purity and thickness of electrode were 5%, 80 HV_{0.05}, 99.99% and 2 mm, respectively.

Low plasticity materials break or crack under stress; they are brittle. They become more fragile when the temperature decreases. Materials with high plasticity rate undergo deformation without breaking or cracking and are ductile, and as the temperature increases, these properties increase further.

The thickness of the Pt layer coated on the Ti layer by the electrodeposition process was $2 \mu\text{m}$ (Fig. 2).

It is clear from Fig. 2 that the Pt layer is thinner than the Ti layer, so the deposition process was carried out successfully. Figure S1(a) (Online Resource 2) shows the SEM image of the bent form of the Ti/Pt electrode. Despite bending, Fig. S1(b) (Online Resource 2) shows almost a smooth surface structure. The high plasticity of the Ti/Pt anode allowed the formation of prism-like structures instead of the brittle mud crack appearance of anode materials with low plasticity. Thus, it can be said that the material has high mechanical and physical strength thanks to its high plasticity.

CCD experiments and findings

CCD experiments designed by the program were carried out to determine the effects of the parameters [initial wastewater pH, J (mA/cm²), Q (mL/min) and SE concentration (mM)] on the removal of COD (%). Removal yields of COD (as a response) for each experiment are presented in the experiment design proposed by CCD (Table 2). The model equations provided by the program are suggested for COD removal yield with regard to coded and uncoded values as noted in Eqs. 6 and 7, respectively:

$$\begin{aligned}
 \text{COD removal}(\%)(\text{uncoded}) = & -28.73110 + 42.04158[\text{pH}] + 1.31190[J] - 0.17396[Q] \\
 & + 0.19644[\text{SE conc.}] + 3.61905E - 003[\text{pH}][J] - 0.055214[\text{pH}][Q] \\
 & - 9.00794E - 003[\text{pH}][\text{SE conc.}] + 9.09167E - 003[J][Q] \\
 & - 8.07407E - 004[J][\text{SE conc.}] + 4.55556E - 004[Q][\text{SE conc.}] \\
 & - 3.78902[\text{pH}^2] - 0.030086[J^2] + 8.82758E - 004[Q^2] \\
 & - 3.58227E - 004[\text{SE conc.}^2]
 \end{aligned} \tag{6}$$



Table 2 CCD experimental set and results

Run	pH, (A)	J (mA/cm ²), (B)	Q (mL/min), (C)	SE Conc. (mM), (D)	COD Removal (%), (Y_o)	COD Removal (%), (Y_p)	ε ($Y_o - Y_p$)
1	2.00 (-1)	20.00 (+1)	50.00 (+1)	10.00 (-1)	50.54	52.44	-1.90
2	2.00 (-1)	20.00 (+1)	50.00 (+1)	100.00 (+1)	69.00	67.55	1.45
3	5.50 (0)	12.50 (0)	30.00 (0)	5.50 (- α)	88.15	89.52	-1.37
4	9.00 (+1)	5.00 (-1)	10.00 (-1)	100.00 (+1)	51.12	50.54	0.58
5	5.50 (0)	20.75 (+ α)	30.00 (0)	55.00 (0)	99.01	99.50	-0.49
6	9.00 (+1)	20.00 (+1)	50.00 (+1)	100.00 (+1)	42.74	43.96	-1.22
7	5.50 (0)	12.50 (0)	30.00 (0)	55.00 (0)	98.45	96.89	1.56
8	2.00 (-1)	5.00 (-1)	10.00 (-1)	100.00 (+1)	59.33	58.05	1.28
9	2.00 (-1)	20.00 (+1)	10.00 (-1)	100.00 (+1)	65.21	65.71	-0.50
10	9.00 (+1)	20.00 (+1)	10.00 (-1)	100.00 (+1)	61.10	59.58	1.52
11	1.65 (- α)	12.50 (0)	30.00 (0)	55.00 (0)	46.59	47.45	-0.86
12	5.50 (0)	12.50 (0)	30.00 (0)	55.00 (0)	98.80	97.56	1.24
13	2.00 (-1)	5.00 (-1)	50.00 (+1)	100.00 (+1)	50.55	51.43	-0.88
14	9.00 (+1)	5.00 (-1)	50.00 (+1)	10.00 (-1)	20.12	20.94	-0.82
15	9.00 (+1)	5.00 (-1)	10.00 (-1)	10.00 (-1)	44.71	43.66	1.05
16	9.35 (+ α)	12.50 (0)	30.00 (0)	55.00 (0)	30.96	31.02	-0.06
17	5.50 (0)	12.50 (0)	30.00 (0)	55.00 (0)	99.01	98.88	0.13
18	9.00 (+1)	20.00 (+1)	10.00 (-1)	10.00 (-1)	53.35	53.79	-0.44
19	2.00 (-1)	20.00 (+1)	10.00 (-1)	10.00 (-1)	58.06	55.24	2.82
20	9.00 (+1)	20.00 (+1)	50.00 (+1)	10.00 (-1)	38.75	36.53	2.22
21	5.50 (0)	12.50 (0)	30.00 (0)	55.00 (0)	98.20	97.12	1.08
22	5.50 (0)	12.50 (0)	52.00 (+ α)	55.00 (0)	90.75	91.03	-0.28
23	2.00 (-1)	5.00 (-1)	10.00 (-1)	10.00 (-1)	44.39	45.49	-1.10
24	5.50 (0)	12.50 (0)	8.00 (- α)	55.00 (0)	99.98	99.78	0.20
25	9.00 (+1)	5.00 (-1)	50.00 (+1)	100.00 (+1)	30.15	29.47	0.68
26	2.00 (-1)	5.00 (-1)	50.00 (+1)	10.00 (-1)	40.22	39.24	0.98
27	5.50 (0)	12.50 (0)	30.00 (0)	55.00 (0)	99.06	98.99	0.07
28	5.50 (0)	4.25 (- α)	30.00 (0)	55.00 (0)	86.77	88.18	-1.41
29	5.50 (0)	12.50 (0)	30.00 (0)	55.00 (0)	98.75	97.89	0.86
30	5.50 (0)	12.50 (0)	30.00 (0)	104.50 (+ α)	99.97	99.99	-0.02

ε corresponded error; Y_o , Y_p observed and predicted response, respectively

$$\begin{aligned} \text{COD removal (\%)(coded)} = & +96.89 - 6.10[A] + 6.06[B] - 5.72[C] + 5.00[D] + 0.095[A][B] \\ & - 3.86[A][C] - 1.42[A][D] + 1.36[B][C] - 0.27[B][D] \\ & + 0.41[C][D] - 46.42[A^2] - 1.69B^2 + 0.35[C^2] - 0.73[D^2] \end{aligned} \quad (7)$$

Effect of operation parameters on removal efficiency

As with all experimental systems, all internal and external parameters affect system efficiency. Determining the parameters that affect system efficiency the most and even determining the degree of effect of the parameters are very important in experimental optimization. It is possible to determine the degree of effect of the parameters with ANOVA analysis. The linear, interaction and quadratic effects of operational

parameters affect the system efficiency to varying degrees. A, B, C, D show linear effects, AB, AC, AD, BC, BD, CD show interaction effects, and A^2 , B^2 , C^2 , D^2 represent quadratic effects of parameters. To observe these effects, ANOVA results are given in Table 3.

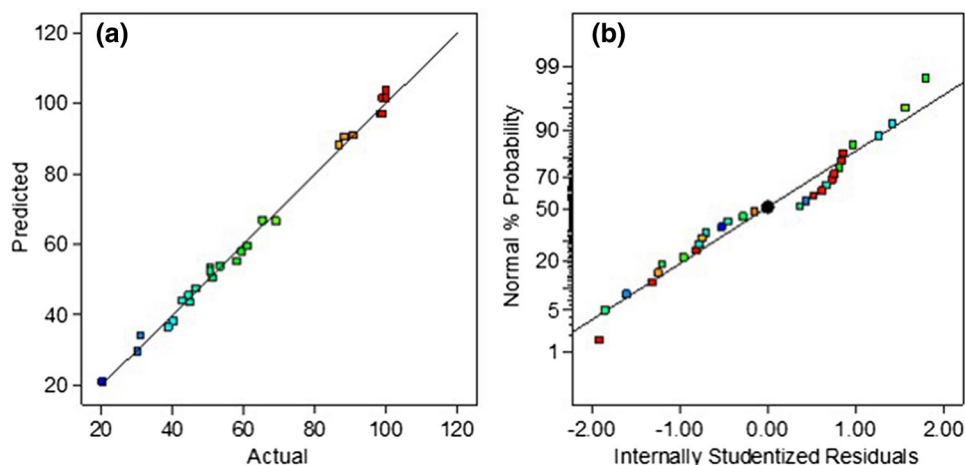
The significance of each term in the quadratic model should be stated via the F value and p value. The model F value of 202.08 implies the model is significant. There is only a 0.01% chance that a “Model F -value” this large could occur due to noise. Rajkumar and Muthukumar (2012)



Table 3 Analysis of variance table for response surface quadratic model

	Sum of squares	Df	Mean square	F value	p value, Prob > F
Model	20,072.74	14	1433.77	202.08	<0.0001
A-pH	686.52	1	686.52	96.76	<0.0001
B-J	676.43	1	676.43	95.34	<0.0001
C-Q	602.57	1	602.57	84.93	<0.0001
D-SE conc.	460.12	1	460.12	64.85	<0.0001
AB	0.14	1	0.14	0.02	0.8885
AC	239.01	1	239.01	33.69	<0.0001
AD	32.21	1	32.21	4.54	0.0501
BC	29.76	1	29.76	4.19	0.0585
BD	1.19	1	1.19	0.17	0.6882
CD	2.69	1	2.69	0.38	0.5473
A ²	8049.11	1	8049.11	1134.45	<0.0001
B ²	10.70	1	10.70	1.51	0.2383
C ²	0.47	1	0.47	0.066	0.8013
D ²	1.97	1	1.97	0.28	0.6063
Pure error	0.55	5	0.11		
Lack of fit	105.88	10	10.59	96.27	0.6673
SD: 2.66					
R ² 0.9947					

Df degrees of freedom

Fig. 3 **a** Graph of predicted values versus actual values, **b** validation of the prediction of COD removal residuals versus normal % probability

reported that the great value of F states that the most part of the variation in the response may be expressed with the equation of regression. Values of “Prob > F ” less than 0.0500 indicate model terms are significant. In this case, A, B, C, D, AC, A² are significant model terms. Values greater than 0.1000 indicate the model terms are not significant. Also, the value of 96.27 for “lack of fit F value” implies that the lack of fit was not significant relative to the pure error. Insignificant lack of fit was good and shows the model was suitable to estimate the removal percentage of BR13 within the explored range of variables.

The coefficient determined for the model is 0.9947, close to 1 (Table 3). This shows that there is a good correlation

between the values predicted by the model and the experimentally obtained values (Fig. 3a). In addition, this implies that 99.47% of the variation in percent COD removal is expressed by the independent variables; in addition, this also means that the model does not express only about 0.53% of the variation. As can be seen from Fig. 3a, the experimentally obtained (actual) values and the values estimated by the model are located close to each other above the graph line. This shows that the values predicted by the model largely represent experimental data and that the model is reliable. The normal probability plots for the residuals are shown in Fig. 3b. Plots in Fig. 3b indicate that the residuals mostly fall along a line, indicating that errors dispersed normally. This

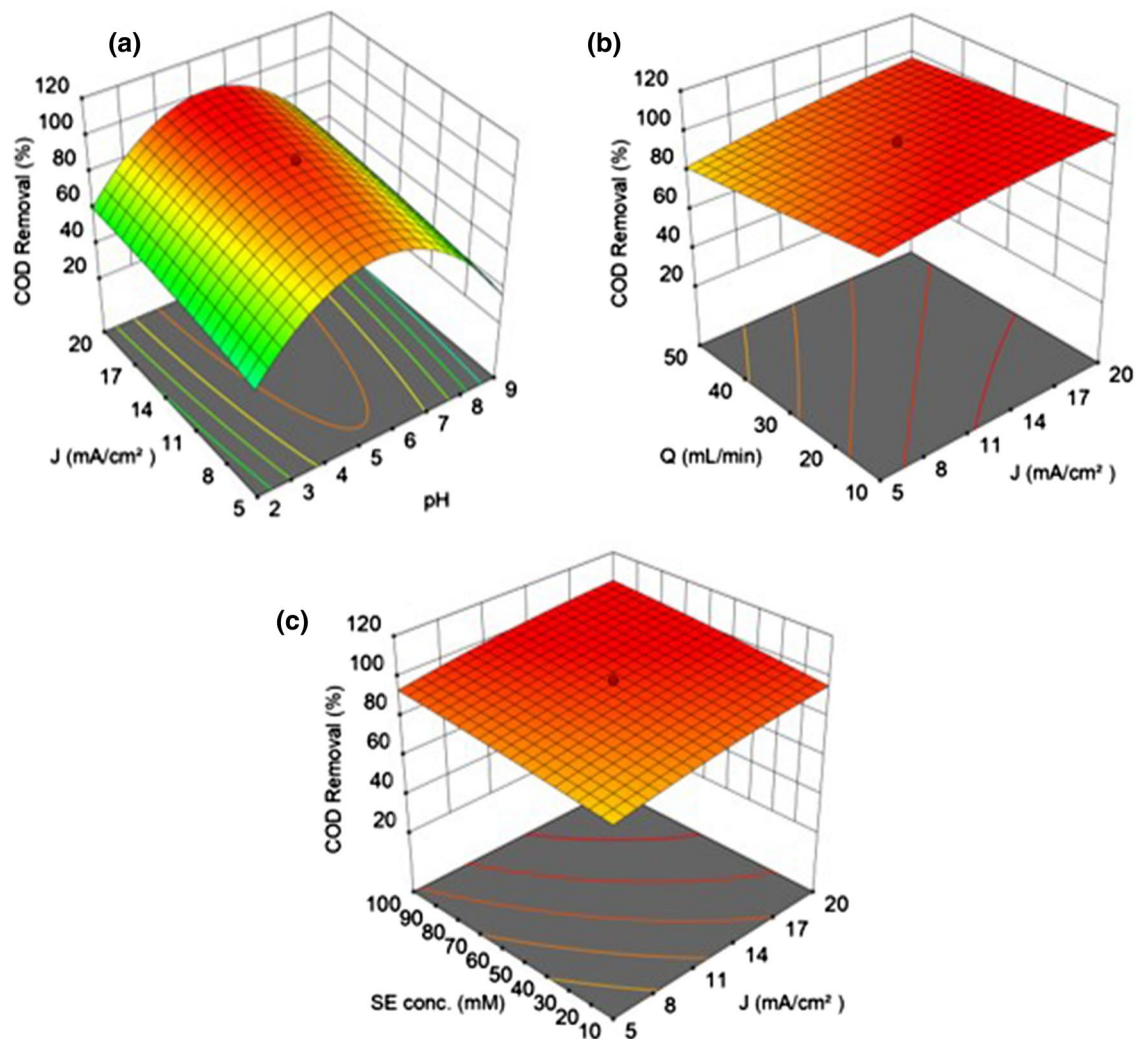


Fig. 4 Combined effects of **a** J and pH, **b** Q and J , **c** SE concentration and J on COD removal yield

shows that the model suggested is satisfactory and there is no occasion to doubt any nonobservance.

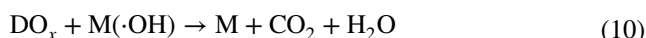
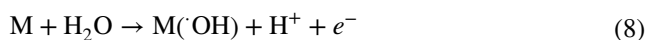
Also, to appraise the statistical sufficiency of the results, the Box–Cox analysis can be examined (Online Resource 3, Fig. S2). As seen in Fig. S2 (Online Resource 3), the minimum confidence interval value is 0.69 and the maximum value is 1.62. The current point of confidence interval ($\lambda = 1$) almost meets the model design value (best = 1.14); as a result, no power transformation of the model was needed as proposed by the Box–Cox analysis.

Three-dimensional graphs indicating the combined effects of the operational parameters that were provided by CCD experiments are given in Fig. 4. The curvature of the plots shows the density of the interaction between the operational parameters. The interaction of the CD–pH (at fixed Q of 30 mL/min, SE concentration of 55 mM), shown in Fig. 4a, shows a substantial relationship between COD removal (%) and both CD–pH. As can be seen from Fig. 4a,

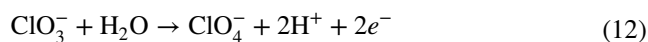
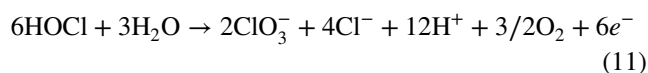
the COD removal efficiency increased approximately twice as the CD increased from 5 to 20 mA/cm². As CD increases, the oxidants produced increase (Maljaei et al. 2009), but if more CD is applied to the solution, it results in parasitic reactions which cause the depletion of hypochlorite concentration (Szpyrkowicz et al. 2005; Mohan et al. 2007). According to the results, the removal yield of COD was above 30% even at lower CDs. This situation suggests that oxidation depends on the type of anode and it might be carried out via both direct and indirect oxidations where there is oxidation of contaminants via electrons transposed to the anode surface and oxidation with electro-produced hydroxyl radicals ($\cdot\text{OH}$) formed from wastewater at the anode surface (M) (Eq. 8) (Tavares et al. 2012), respectively. The efficiency of the $\cdot\text{OH}$ radicals is associated with their interplay with the anode surface (M). While the degradation of organic substances is mainly related to applied CD, the type of electrode is efficient. Ti/Pt electrodes are classified as active anodes



(Martínez-Huitle and Ferro 2006; Panizza and Cerisola 2009). A low quantity of reactive $M(\cdot OH)$ is formed by oxidation at the Ti/Pt electrodes (Lahkimi et al. 2007; Panizza et al. 2007; Martínez-Huitle and Brillas 2009). The potent interaction between M and $\cdot OH$ and low O_2 evolution over potential makes oxidation of the weaker MO_x species possible (Fajardo et al. 2017). Produced chemisorbed oxygen (MO_x) assists the fractional reduction in the dyes (D) (Eq. 9) (Tavares et al. 2012). Finally, partly oxidized organic matter (DO_x) is oxidized again by the low amount of $M(\cdot OH)$ radicals produced. The complete oxidation of such complex synthetic dye molecules to CO_2 and H_2O is possible with low probability (Rajkumar et al. 2007). However, almost all of them can be oxidized to very small molecules (P) and CO_2 and H_2O are produced as byproducts in the final step (Eq. 10) (Martínez-Huitle and Panizza 2018):



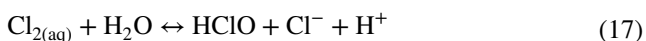
Also, the effect of the initial pH of solution on removal efficiency is observed in Fig. 4a. When the initial pH value of the solution increased from 2 to 5.5, the removal efficiency of COD reached almost 100%. This can be explained as follows: In acidic pH, oxidants are dominant such as $Cl_{2(aq)}$, $HOCl$ and $\cdot OH$ (Pletcher and Walsh 1999; Deborde and Von Gunten 2008) and the high removal of COD is due to oxidation mediated by Cl_2 and $HOCl$ and direct oxidation by sorbed $\cdot OH$ on the surface of anode. Furthermore, in acidic pH there is also proof of the presence of other reactive types in the EO (Akrouf et al. 2015). $HClO$ is the dominant reactive species for the reaction with the generality of organic compounds (Deborde and Von Gunten 2008). Because of its oxidizing potency, there are three types of reactions: addition to unsaturated bonds, substitution to nucleophilic sites and oxidation. In the presence of dye molecules, the oxidation consists preferably of the substituents of aromatic rings. When the pH value increased from 5.5 to 9, the removal efficiency suddenly decreased by nearly 30%. At high pH (above 7), chloro-active species OCl^- (0.94 V) are predominant which have lower oxidation potential than $HOCl$ (1.49 V) and $\cdot OH$. Due to the formation of ClO_3^- or ClO_4^- (Eqs. 11 and 12) (Kim and Park 2012), the production of $Cl_2/HOCl$ decreased. Therefore, removal of COD is performed with oxidation mediated by HO_2 and H_2O_2 and OCl^- . Also, the sorption percentage of $\cdot OH$ on the surface of the anode decreases with increasing pH and generated $\cdot OH$ is turned into H_2O_2 and HO_2 (Eqs. 13 and 14) (Zaharia et al. 2009) which have lower oxidation potential:



The interaction of the $Q-J$ (at a fixed pH of 5.50, SE concentration of 55 mM), shown in Fig. 4b, shows a substantial correlation between the COD removal (%) and Q . This disclosure does not exclude the significant impact of CD on removal efficiency, but emphasizes the importance of Q in removal efficiency with increasing acceleration. When Q decreased from 50 mL/min to 10 mL/min, COD removal efficiency increased rapidly from about % 82 to over % 90. As Q increases, the reaction time is shortened and the pollutants leave the system without sufficient electrochemical degradation. Moreover, due to the nature of continuous flow electrochemical systems, mixing effects occur. This effect contributes to the mixing of the solution and so positively affects the mass transfer. For this reason, it is necessary to determine the required hydraulic retention times in order to ensure full contact of the oxidants and pollutants during EO.

The interaction of the $SE-J$ (at fixed pH of 5.50, Q of 30 mL/min) is shown in Fig. 4c. As seen from Fig. 4c, the degradation rate of pollutants increased with NaCl concentration positively, depending on mediated oxidation. It is well known that electrolysis of chloride solutions in divided cells involves the direct oxidation of Cl^- , to supply soluble Cl_2 (Eq. 15) (Tavares et al. 2012). There is a reduction in H_2O at the cathode which supplies OH^- and $H_{2(g)}$. If the concentration of chlorine is greater than its solubility, oversaturation ensures the generation of $Cl_{2(g)}$ bubbles (Tavares et al. 2012). Because the electro-generated chlorine moves away from the anode, trichloride ions can develop from its reaction with chloride ions (Eq. 16) (Tavares et al. 2012). Another possibility is transformations of chlorine to chloride ions and hypochlorous acid due to hydrolyzation (Eq. 17) (Tavares et al. 2012). Hypochlorite ion and hypochlorous acid are in balance via reversible reaction (Eq. 18) (Tavares et al. 2012). Oxidative species can change with pH. This species is soluble chlorine at pH 3, is hypochlorous acid at pH from 3 and 8 and is hypochlorite ions above pH 8 (Tavares et al. 2012). Additionally, chlorate can occur based on operating conditions, which can assist the oxidation of organic substances indirectly (Eq. 19) (Tavares et al. 2012).





During mediated oxidation, an increase in NaCl concentration leads to a gradual modification of the oxygen exchange reaction to more suitable potentials compared to electrolysis in the absence of SE (Ozturk and Yilmaz 2019). Similar comments are presented in the literature (Panizza and Cerisola 2003; Fernandes et al. 2004; Tavares et al. 2012). As can be seen from Fig. 4c, even at a low salt concentration (10 mM), the lowest removal efficiency is above 75%, and with increasing salt concentration the removal efficiency is increased with increasing acceleration. This is likely owing to the nature of NaCl which produces potent oxidants that may contribute to mediated dye removal.

Numerical optimization of results

Hundreds of experiments are required for the optimization of parameters affecting experimental systems performed by conventional methods. However, by using optimization procedures such as RSM, it is possible to considerably reduce the number of experiments (in parallel with chemical consumption, time and labor) and maximize the result. In this study, it was possible to provide system optimization with thirty experiments. Using numerical optimization, the desired value can be selected for each input factor and response. Here, the possible optimization entries that can be selected include: range, maximum, minimum, target, none (for responses) and be set to generate an optimized output value for a given set of conditions. The chosen target for pH and COD removal yield (%) were fixed as 4.38 (to reduce chemical consumption in possible industrial applications) and 99.98 (max observed yield value), respectively. Q and SE concentration criteria were selected in the ranges. The most appropriate alternative optimization results offered by the system for each parameter according to the selected parameter values are given in Table 4.

Table 4 Solutions for system optimization offered by RSM

Solution	J (mA/cm ²)	Q (mL/min)	SE Conc. (mM)	Y_p (%)	Y_o (%)	E (kW h/m ³)	SEC (kW h/kg COD)
1	19.53	40.78	85.57	99.98	99.95	7.91	0.98
2	17.51	10.35	44.86	99.98	99.93	26.50	3.21
3	10.93	11.18	77.96	99.98	99.90	15.31	1.86
4	15.74	24.00	77.21	99.98	99.94	10.67	1.29
5	16.66	17.10	59.65	99.98	99.89	15.06	1.83

Although multiple alternative sets are offered for system optimization, energy consumption is an important limiting factor in systems using electricity such as electro-oxidation. For this reason, a reasonable optimization set should be chosen where removal efficiency is high, but the energy consumption is low. Accordingly, the first solution presented in Table 4 was deemed appropriate. However, the concentration of the electrolyte (85.57 mM) used is a handicap for the first solution to be deemed appropriate. What should be considered at this time is whether the electricity consumption or the cost of NaCl will be lower. According to market research, 1 ton NaCl (99.99% purity) in 2019 is approximately \$42. Also, the average electricity price is 13.19 cents/kW-h in September 2019. In light of these data, the first solution with the lowest energy consumption and the second solution with the lowest NaCl were evaluated in terms of cost for the treatment of one ton of wastewater. According to the calculations, the amount of NaCl consumed in the first solution was calculated as 0.05 tons (to provide the concentration of NaCl as 85.57 mM) and the amount of NaCl consumed for the second solution was calculated approximately as 0.03 tons (to provide the concentration of NaCl as 44.86 mM). The results are given in Table 5.

As can be seen from Table 5, the energy cost is much more important than the cost of NaCl consumption. Therefore, since NaCl is inexpensive and electricity costs are high, the most appropriate optimization conditions can be considered to be the first solution in terms of both removal efficiency and system cost for optimum system conditions. Due to the fact that the degradation of BR13 is best in acidic pH and the solution pH of BR13 is 4.38 (native value of dye solution), no extra chemicals will be required for pH adjustment. Thus, according to the first solution, when an industrial system is operated, the COD yield will be 99.98% and

Table 5 Cost calculations for the proposed optimization of solutions

Solution	Energy cost (depending on NaCl usage)(\$)	Energy cost (depending on electricity usage) (\$)	Total cost (\$)
1	0.21	1.04	1.25
2	0.11	3.50	3.61



Table 6 Studies on the treatment of wastewater containing dye by electro-oxidation method using Ti/Pt electrodes

Dye	J (mA/cm ²)	COD removal (%)	SEC (kW h/kg COD)	E (kW h/m ³)	References
Azo dyeing process wastewater	890	86	21	–	Vlyssides et al. (1999)
Methylene Blue	50	> 80	–	33.60	de Oliveira et al. (2011)
Novacron Yellow	40	> 50	30.31	–	Araújo et al. (2014)
Remazol Red	40	< 25	–	31.20	Araújo et al. (2014)
Reactive Orange 4	24	81	–	698	López-Grimau and Gutierrez (2006)
Basic Red 13 (BR13)	19.53	99.98	0.98	7.91	This study

the approximate cost of the system to treat 1 ton of wastewater will be \$1.25.

One of the most important ways of understanding the place of a scientific study in the literature is to examine previous studies in the related field. Several studies on the treatment of wastewater containing dye by EO method using Ti/Pt electrodes are shown in Table 6.

It is seen from Table 6 that dye-containing wastewaters can be successfully treated using Ti/Pt electrodes. The issue that limits the applicability of these studies is energy consumption values. There are many factors that affect energy consumption (use of support electrolytes, reaction time, current density, etc.). CD is one of the most important factors affecting energy consumption. Curteanu et al. (2011) reported that the CD applied at high values causes an increase in the potential difference. Therefore, if the CD rises above the optimum value, a large part of the current applied to the system causes the temperature of the degraded organic pollutant in the wastewater to rise, wasting energy and thus uneconomical. Similar comments made by Hamad et al. (2018). However, this effect of current density can be reduced by changing some operational conditions. The use of support electrolyte and shortening of the reaction time are good examples. Salazar et al. (2018) reported that the use of NaCl is very effective both in reducing the reaction time and in reducing the energy consumption in the system. There are many other parameters (type and chemical structure of pollutants, design of the reactor, the hydraulic retention time of wastewater, connection types of electrodes, etc.) that reduce and increase energy consumption in the system (Nava et al. 2008). Optimization of such parameters is very important both in terms of removal efficiency and minimization of energy consumption. As can be seen from Table 6, it is clear that in this study there are lower current density, higher removal efficiency and lower energy consumption values observed than other studies. The subject that distinguishes this study from other studies is the optimization of some parameters affecting the system with the optimization program apart from classical experimental methods. Thus,

optimum points were successfully determined for low energy consumption and high removal efficiency.

Conclusion

Results of oxidation of the water-soluble Basic Red 13 dye by electro-oxidation at room temperature in an electrochemical reactor with a titanium cathode and a platinized titanium anode as monitored by COD measurements indicated almost complete degradation (approximately 99.98%) of the dye. EO process performance increased with increased NaCl concentration according to an increase in the concentration of active chlorine species in solution.

According to numerical optimization results, degradation of BR13 was the best in acidic conditions (4.38 as native pH of dye solution). To achieve low cost and high removal efficiency, the optimal points for applied current density, flow rate and supporting electrolyte concentration were determined as 19.53 mA/cm², 40.78 mL/min and 85.57 mM, respectively, by numeric optimization. At these optimum points, the energy consumption of the system was calculated as 7.91 kW h/m³ and 0.98 kW h/kg COD. Under these conditions when an industrial system is operated, the approximate cost of the system to treat 1 ton of wastewater will be \$1.25.

Acknowledgements The authors would like to thank Mustafa Goktepe, Galtek Kimya Metal Plastik Makine San. Tic. Ltd. Şti. and Umicore for their help in providing the electrodes and their help in analyses of SEM, EDX and plasticity of electrodes.

References

- Ademoroti CMA (1996) Standard method for water and effluent analysis. March Prints and Consultancy, Foludex Press Limited, Ibadan, p 182
- Akrouit H, Jellali S, Bousselmi L (2015) Enhancement of methylene blue removal by anodic oxidation using BDD electrode combined with adsorption onto sawdust. *CR Chim* 18:110–120. <https://doi.org/10.1016/j.crci.2014.09.006>

- Anglada A, Urtiaga A, Ortiz I (2009) Contributions of electrochemical oxidation to waste-water treatment: fundamentals and review of applications. *J Chem Technol Biotechnol* 84(12):1747–1755. <https://doi.org/10.1002/jctb.2214>
- Araújo CK, Oliveira GR, Fernandes NS, Zanta CL, Castro SSL, da Silva DR, Martínez-Huitle CA (2014) Electrochemical removal of synthetic textile dyes from aqueous solutions using Ti/Pt anode: role of dye structure. *Environ Sci Pollut Res* 21(16):9777–9784. <https://doi.org/10.1007/s11356-014-2918-4>
- Assémian AS, Kouassi KE, Drogui P, Adouby K, Boa D (2018) Removal of a persistent dye in aqueous solutions by electrocoagulation process: modeling and optimization through response surface methodology. *Water Air Soil Pollut* 229(6):184. <https://doi.org/10.1007/s11270-018-3813-2>
- Atmaca E (2009) Treatment of landfill leachate by using electro-Fenton method. *J Hazard Mater* 163(1):109–114. <https://doi.org/10.1016/j.jhazmat.2008.06.067>
- Azarian G, Miri M, Nematollahi D (2018) Combined electrocoagulation/electrooxidation process for the COD removal and recovery of tannery industry wastewater. *Environ Prog Sustain Energy* 37(2):637–644. <https://doi.org/10.1002/ep.12711>
- Bahia M, Passos F, Adarme OF, Aquino SF, Silva SQ (2018) Anaerobic-aerobic combined system for the biological treatment of azo dye solution using residual yeast. *Water Environ Res* 90(8):729–737. <https://doi.org/10.2175/106143017X15131012153167>
- Brillas E, Martínez-Huitle CA (2015) Decontamination of wastewaters containing synthetic organic dyes by electrochemical methods. An updated review. *Appl Catal B Environ* 166:603–643. <https://doi.org/10.1016/j.apcatb.2014.11.016>
- Curteanu S, Piuleac CG, Godini K, Azaryan G (2011) Modeling of electrolysis process in wastewater treatment using different types of neural networks. *Chem Eng J* 172(1):267–276. <https://doi.org/10.1016/j.cej.2011.05.104>
- de Oliveira GR, Fernandes NS, de Melo JV, da Silva DR, Urgeghe C, Martínez-Huitle CA (2011) Electrocatalytic properties of Ti-supported Pt for decolorizing and removing dye from synthetic textile wastewaters. *Chem Eng J* 168(1):208–214. <https://doi.org/10.1016/j.cej.2010.12.070>
- Deborde M, Von Gunten URS (2008) Reactions of chlorine with inorganic and organic compounds during water treatment—kinetics and mechanisms: a critical review. *Water Res* 42(1–2):13–51. <https://doi.org/10.1016/j.watres.2007.07.025>
- Dick GB (1990) Electroplating with platinum by high temperature electrolysis. *Oberfläche Surf* 31(3):8–12
- Dotto J, Fagundes-Klen MR, Veit MT, Palácio SM, Bergamasco R (2019) Performance of different coagulants in the coagulation/flocculation process of textile wastewater. *J Clean Prod* 208:656–665. <https://doi.org/10.1016/j.jclepro.2018.10.112>
- Eaton AD, Clesceri LS, Greenberg AE, Franson MAH (1995) Standard methods for the examination of water and wastewater. American Public Health Assoc (APHA) Inc, New York
- Fajardo AS, Martins RC, Silva DR, Quinta-Ferreira RM, Martínez-Huitle CA (2017) Electrochemical abatement of amaranth dye solutions using individual or an assembly of flow cells with Ti/Pt and Ti/Pt–SnSb anodes. *Sep Purif Technol* 179:194–203. <https://doi.org/10.1016/j.seppur.2017.01.029>
- Fernandes A, Morao A, Magrinho M, Lopes A, Gonçalves I (2004) Electrochemical degradation of CI acid orange 7. *Dyes Pigment* 61(3):287–296. <https://doi.org/10.1016/j.dyepig.2003.11.008>
- Gharbani P, Tabatabaï SM, Mehrizad A (2008) Removal of Congo red from textile wastewater by ozonation. *Int J Environ Sci Technol* 5(4):495–500. <https://doi.org/10.1007/BF03326046>
- Hamad H, Bassyouni D, El-Ashtoukhy ES, Amin N, El-Latif MA (2018) Electrocatalytic degradation and minimization of specific energy consumption of synthetic azo dye from wastewater by anodic oxidation process with an emphasis on enhancing economic efficiency and reaction mechanism. *Ecotoxicol Environ Saf* 148:501–512. <https://doi.org/10.1016/j.ecoenv.2017.10.061>
- Hassani AH, Mirzayee R, Nasseri S, Borghei M, Gholami M, Torabifar B (2008) Nanofiltration process on dye removal from simulated textile wastewater. *Int J Environ Sci Technol* 5(3):401–408. <https://doi.org/10.1007/BF03326035>
- İlgin P, Ozay O (2017) Novel stimuli-responsive hydrogels derived from morpholine: synthesis, characterization and absorption uptake of textile azo dye. *Iran Polym J* 26(6):391–404. <https://doi.org/10.1007/s13726-017-0528-y>
- Kaykioglu G, Debik E (2006) Color removal from textile wastewater with anaerobic treatment processes. *Sigma J Eng Nat Sci* 4:59–68
- Khumalo NP, Nthunya LN, De Canck E, Derese S, Verliefdé AR, Kuvarega AT, Mamba BB, Mhlanga SD, Dlamini DS (2019) Congo red dye removal by direct membrane distillation using PVDF/PTFE membrane. *Sep Purif Technol* 211:578–586. <https://doi.org/10.1016/j.seppur.2018.10.039>
- Kim DS, Park YS (2012) COD removal of rhodamine B from aqueous solution by electrochemical treatment. *J Environ Sci Int* 21(6):655–659. <https://doi.org/10.5322/JES.2012.21.6.655>
- Kıvanç MR, Yönten V (2020) A statistical optimization of methylene blue removal from aqueous solutions by *Agaricus campestris* using multi-step experimental design with response surface methodology: Isotherm, kinetic and thermodynamic studies. *Surf Interfaces* 18:100414. <https://doi.org/10.1016/j.surfin.2019.100414>
- Lahkimi A, Oturan MA, Oturan N, Chaouq M (2007) Removal of textile dyes from water by the electro-Fenton process. *Environ Chem Lett* 5(1):35–39. <https://doi.org/10.1007/s10311-006-0058-x>
- López-Grimau V, Gutierrez MC (2006) Decolourisation of simulated reactive dyebath effluents by electrochemical oxidation assisted by UV light. *Chemosphere* 62(1):106–112. <https://doi.org/10.1016/j.chemosphere.2005.03.076>
- Maljaei A, Arami M, Mahmoodi NM (2009) Decolorization and aromatic ring degradation of colored textile wastewater using indirect electrochemical oxidation method. *Desalination* 249(3):1074–1078. <https://doi.org/10.1016/j.desal.2009.05.016>
- Martínez-Huitle CA, Brillas E (2009) Decontamination of wastewaters containing synthetic organic dyes by electrochemical methods: a general review. *Appl Catal B Environ* 87(3–4):105–145. <https://doi.org/10.1016/j.apcatb.2008.09.017>
- Martínez-Huitle CA, Ferro S (2006) Electrochemical oxidation of organic pollutants for the wastewater treatment: direct and indirect processes. *Chem Soc Rev* 35(12):1324–1340
- Martínez-Huitle CA, Panizza M (2018) Electrochemical oxidation of organic pollutants for wastewater treatment. *Curr Opin Electrochem* 11:62–71. <https://doi.org/10.1016/j.coelec.2018.07.010>
- Mohan N, Balasubramanian N, Basha CA (2007) Electrochemical oxidation of textile wastewater and its reuse. *J Hazard Mater* 147(1–2):644–651. <https://doi.org/10.1016/j.jhazmat.2007.01.063>
- Nava JL, Quiroz MA, Martínez-Huitle CA (2008) Electrochemical treatment of synthetic wastewaters containing alphanurine a dye: role of electrode material in the colour and COD removal. *J Mex Chem Soc* 52(4):249–255
- Öztürk D, Şahan T (2015) Design and optimization of Cu(II) adsorption conditions from aqueous solutions by low-cost adsorbent pumice with response surface methodology. *Pol J Environ Stud* 24(4):1749–1756. <https://doi.org/10.15244/pjoes/40270>
- Ozturk D, Yilmaz AE (2019) Treatment of slaughterhouse wastewater with the electrochemical oxidation process: role of operating parameters on treatment efficiency and energy consumption. *J Water Process Eng* 31:100834. <https://doi.org/10.1016/j.jwpe.2019.100834>
- Ozturk D, Şahan T, Bayram T, Erkus A (2017) Application of response surface methodology (RSM) to optimize the adsorption conditions of cationic basic yellow 2 onto pumice samples as a new adsorbent. *Fresen Environ Bull* 26(5):3285–3292



- Panizza M, Cerisola G (2003) Electrochemical oxidation of 2-naphthol with in situ electrogenerated active chlorine. *Electrochim Acta* 48(11):1515–1519. [https://doi.org/10.1016/S0013-4686\(03\)00028-8](https://doi.org/10.1016/S0013-4686(03)00028-8)
- Panizza M, Cerisola G (2009) Direct and mediated anodic oxidation of organic pollutants. *Chem Rev* 109(12):6541–6569. <https://doi.org/10.1021/cr9001319>
- Panizza M, Barbucci A, Ricotti R, Cerisola G (2007) Electrochemical degradation of methylene blue. *Sep Purif Technol* 54(3):382–387. <https://doi.org/10.1016/j.seppur.2006.10.010>
- Pletcher D, Walsh FC (1999) *Industrial electrochemistry*, vol XII. Chapman and Hall, London, p 325
- Qada ENE, Aleen SJ, Walker GM (2006) Adsorption of methylene blue onto activated carbon produced from steam activated bituminous coal: a study of equilibrium isotherm. *Chem Eng J* 124:103–110. <https://doi.org/10.1016/j.cej.2006.08.015>
- Rahmani AR, Godini K, Nematollahi D, Azarian G (2015) Electrochemical oxidation of activated sludge by using direct and indirect anodic oxidation. *Desalin Water Treat* 56(8):2234–2245. <https://doi.org/10.1080/19443994.2014.958761>
- Rajkumar K, Muthukumar M (2012) Optimization of electro-oxidation process for the treatment of reactive orange 107 using response surface methodology. *Environ Sci Pollut Res* 19(1):148–160. <https://doi.org/10.1007/s11356-011-0532-2>
- Rajkumar D, Song BJ, Kim JG (2007) Electrochemical degradation of reactive blue 19 in chloride medium for the treatment of textile dyeing wastewater with identification of intermediate compounds. *Dyes Pigment* 72(1):1–7. <https://doi.org/10.1016/j.dyepig.2005.07.015>
- Salazar R, Ureta-Zañartu MS, González-Vargas C, do Nascimento Brito C, Martínez-Huitle CA (2018) Electrochemical degradation of industrial textile dye disperse yellow 3: role of electrocatalytic material and experimental conditions on the catalytic production of oxidants and oxidation pathway. *Chemosphere* 198:21–29. <https://doi.org/10.1016/j.chemosphere.2017.12.092>
- Sarvajith M, Reddy GKK, Nancharaiah YV (2018) Textile dye biodecolourization and ammonium removal over nitrite in aerobic granular sludge sequencing batch reactors. *J Hazard Mater* 342:536–543. <https://doi.org/10.1016/j.jhazmat.2017.08.064>
- Şen F, Demirbaş Ö, Çalimli MH, Aygün A, Alma MH, Nas MS (2018) The dye removal from aqueous solution using polymer composite films. *Appl Water Sci* 8(7):206. <https://doi.org/10.1007/s13201-018-0856-x>
- Szpyrkowicz L, Kaul SN, Neti RN (2005) Tannery wastewater treatment by electro-oxidation coupled with a biological process. *J Appl Electrochem* 35(4):381–390. <https://doi.org/10.1007/s10800-005-0796-7>
- Takdastan A, Tabar SE, Islam A, Bazafkan MH, Naisi AK (2015) The effect of the electrode in fluoride removal from drinking water by electro coagulation process. In: *International conference on chemical, environmental and biological science (CEBS-2015)*, pp 39–44. <http://dx.doi.org/10.15242/IICBE.C0315073>
- Tavares MG, da Silva LV, Solano AMS, Tonholo J, Martínez-Huitle CA, Zanta CLPS (2012) Electrochemical oxidation of methyl red using Ti/RuO₂·3TiO₂·7O₂ and Ti/Pt anodes. *Chem Eng J* 204:141–150. <https://doi.org/10.1016/j.cej.2012.07.056>
- Tiaiba M, Merzouk B, Mazour M, Leclerc JP, Lapique F (2018) Study of chemical coagulation conditions for a disperse red dye removal from aqueous solutions. *Membr Water Treatment* 9(1):9–15. <https://doi.org/10.12989/mwt.2018.9.1.009>
- Venkatesh S, Venkatesh K (2019) Ozonation for degradation of acid red 14: effect of buffer solution. *Proc Natl Acad Sci India Sect A Phys Sci*. <https://doi.org/10.1007/s40010-018-0583-6>
- Vignesh A, Siddarth AS, Gokul OS, Babu BR (2014) A novel approach for textile dye degradation by zinc, iron-doped tin oxide/titanium moving anode. *Int J Environ Sci Technol* 11(6):1669–1678. <https://doi.org/10.1007/s13762-013-0318-9>
- Vlyssides AG, Loizidou M, Karlis PK, Zorpas AA, Papaioannou D (1999) Electrochemical oxidation of a textile dye wastewater using a Pt/Ti electrode. *J Hazard Mater* 70(1–2):41–52. [https://doi.org/10.1016/S0304-3894\(99\)00130-2](https://doi.org/10.1016/S0304-3894(99)00130-2)
- Wang S, Boyjoo Y, Choueib A, Zhu ZH (2005) Removal of dyes from aqueous solution using fly ash and red mud. *Water Res* 39(1):129–138. <https://doi.org/10.1016/j.watres.2004.09.011>
- Wang XS, Zhou Y, Jiang Sun C (2008) The removal of basic dyes from aqueous solutions using agricultural by-products. *J Hazard Mater* 157(2–3):374–385. <https://doi.org/10.1016/j.jhazmat.2008.01.004>
- Zaharia C, Suteu D, Muresan A, Muresan R, Popescu A (2009) Textile wastewater treatment by homogenous oxidation with hydrogen peroxide. *Environ Eng Manag J* 8(6):1359–1369
- Zhu X, Ni J, Lai P (2009) Advanced treatment of biologically pre-treated coking wastewater by electrochemical oxidation using boron-doped diamond electrodes. *Water Res* 43(17):4347–4355. <https://doi.org/10.1016/j.watres.2009.06.030>

